Title

Diesel exhaust particles dysregulate multiple immunological pathways in murine macrophages: Lessons from microarray and scRNA-seq technologies

Authors

Bhetraratana, May
Orozco, Luz D
Hong, Jason
et al.

Publication Date

2019-12-01

DOI

10.1016/j.abb.2019.108116

Peer reviewed

HHS Public Access

Author manuscript

Arch Biochem Biophys. Author manuscript; available in PMC 2021 March 23.

Published in final edited form as:

Arch Biochem Biophys. 2019 December 15; 678: 108116. doi:10.1016/j.abb.2019.108116.

Diesel Exhaust Particles Dysregulate Multiple Immunological Pathways in Murine Macrophages: Lessons from Microarray and scRNA-seq Technologies

May Bhetraratana[a], **Luz D. Orozco**[b], **Jason Hong**[c], **Graciel Diamante**[c], **Sana Majid**[c], **Brian J. Bennett**[a], **In Sook Ahn**[c], **Xia Yang**[c,d,e], **Aldons J. Lusis**[a,b,e], **Jesus A. Araujo**[a,e,f]

[a]Division of Cardiology, Department of Medicine, David Geffen School of Medicine at UCLA, Los Angeles, California, USA

[b]Department of Human Genetics, David Geffen School of Medicine at UCLA, Los Angeles, California, USA

[c]Department of Integrative Biology and Physiology, UCLA, Los Angeles, California, USA

[d]Institute for Quantitative and Computational Biosciences, UCLA, Los Angeles, California, USA

[e]Molecular Biology Institute, UCLA, Los Angeles, California, USA.

[f]Department of Environmental Health Sciences, Fielding School of Public Health, UCLA, Los Angeles, California, USA

Abstract

Exposure to ambient particulate matter has been shown to promote a variety of disorders, including cardiovascular diseases predominantly of ischemic etiology. However, the mechanisms linking inhaled particulates with systemic vascular effects, resulting in worsened atherosclerosis, are not well defined. We assessed the potential role of macrophages in translating these effects by analyzing gene expression patterns in response to diesel exhaust particles (DEP) at the average cell level, using Affymetrix microarrays in peritoneal macrophages in culture (in vitro), and at the individual cell level, using single-cell RNA sequencing (scRNA-seq) in alveolar macrophages collected from exposed mice (in vivo). Peritoneal macrophages were harvested from C57BL/6J mice and treated with 25 μg/mL of a DEP methanol extract (DEPe). These cells exhibited significant (FDR < 0.05) differential expression of a large number of genes and enrichment in pathways, especially engaged in immune responses and antioxidant defense. DEPe led to marked upregulation of heme oxygenase 1 (*Hmox1*), the most significantly upregulated gene (FDR = 1.75E-06), and several other antioxidant genes. For the in vivo work, C57BL/6J mice were subjected to oropharyngeal aspiration of 200 μg of whole DEP. The gene expression profiles of the

Corresponding Author: Jesus A. Araujo, MD, PhD. Division of Cardiology, David Geffen School of Medicine at UCLA, 10833 Le Conte Avenue, CHS 43-264, P.O. Box 951679, Los Angeles, CA 90095, USA. Phone number (310) 825-3222, Fax number (310) 206-9133. JAraujo@mednet.ucla.edu.

Present/Permanent Address: Jesus A. Araujo, MD, PhD, Division of Cardiology, David Geffen School of Medicine at UCLA, 10833 Le Conte Avenue, CHS 43-264, P.O. Box 951679, Los Angeles, CA 90095, USA

alveolar macrophages harvested from these mice were analyzed at the single-cell level using scRNA-seq, which showed significant dysregulation of a broad number of genes enriched in immune system pathways as well, but with a large heterogeneity in how individual alveolar macrophages responded to DEP exposures. Altogether, DEP pollutants dysregulated immunological pathways in macrophages that may mediate the development of pulmonary and systemic vascular effects.

Keywords

Macrophages; Air Pollution; Diesel Exhaust Particles; Oxidative Stress; Heme Oxygenase

Taxonomy

Molecular Network; Genes

1. Introduction

Exposure to ambient particulate matter (PM) is associated with adverse health effects, resulting in increased morbidity and mortality worldwide [1]. Diesel exhaust is a major source of particulates in air pollution. Concentrations of diesel exhaust particles (DEP) can be especially high for those in lines of work with heavy vehicular usage such as miners, with estimated occupational exposure levels at 1,280 μg/m^3 of DEP [2]. Even just living around major roadways can be hazardous. For example, people near Wilshire and Sunset Boulevards in Los Angeles may be subjected at times to concentrations around 40 μg/m^3 of $PM_{2.5}$ (PM < 2.5 μm in diameter) [3]. These concentrations are higher than the United States Environmental Protection Agency's 24-hour $PM_{2.5}$ standard of 35 μg/m^3 [4].

PM-induced mortality is largely due to cardiovascular diseases of ischemic etiology [1, 5]. Work with experimental animals has shown that exposure to PM results in enhanced atherosclerosis development [6, 7]. It is unclear, however, how the inhalation of particulates promotes atherosclerosis and cardiovascular diseases. Various pathways have been proposed [1, 8] but the accrued evidence is either inconsistent or too limited to make any definitive conclusions. In the most feasible pathway, inhaled particulates induce oxidative stress and inflammation in the lungs with subsequent expansion into the systemic circulation via release of inflammatory mediators [1, 8]. We have shown that inhaled ambient ultrafine particles can be taken up by alveolar macrophages in the lungs, with predominant localization to the mitochondria [6, 7]. In addition, we and others have shown that an extract of DEP (DEPe), which are highly enriched in organic components, triggers the generation of reactive oxygen species (ROS) in RAW 264.7 macrophages [9], and the synthesis of proinflammatory cytokines in THP-1 cells [10].

Macrophages are critical in the development of inflammatory processes in the lungs and in the cardiovascular system leading to atherosclerosis. Therefore, they are likely candidates to mediate toxic effects induced by inhaled DEP in the lungs that are subsequently carried onto the systemic circulation. In the current study, we aimed to characterize macrophage responses induced by DEP in vitro and in vivo, using transcriptomic approaches in two

models of DEP exposure. Our in vitro work utilized the power of Affymetrix microarrays to elucidate genome-wide changes following treatment of peritoneal macrophages in culture with DEPe. In the in vivo work, we conducted single-cell RNA sequencing (scRNA-seq) to evaluate the responses of individual alveolar macrophages to DEP administered to mice by oropharyngeal aspiration. We utilized peritoneal macrophages in the in vitro experiment because of the ease in acquiring enough cell numbers suitable for cell culture work, while we focused on alveolar macrophages in the in vivo experiment since these cells directly come into contact with instilled particulates. Both approaches (microarray and scRNA-seq) allowed us to identify robust effects on innate immunity and antioxidant pathways as well as to determine the utility of in vitro work in predicting responses induced by air pollutants in vivo.

2. Materials and methods

2.1 Diesel exhaust particles (DEP) and extract (DEPe)

DEP was produced from an ultra-low sulfur highway-grade number 2 diesel fuel by an automobile single cylinder diesel engine from the Yanmar America Corporation [11]. Particles were resuspended in phosphate-buffered saline (PBS) and sonicated for several minutes on ice. Aliquots were made and stored at −80°C until ready to use. For cell culture work, an extract of DEP (DEPe) was made via methanol extraction as described previously [10] with a yield recovery of ~80%, consistent with other studies where the organic components are reported to constitute as little as 20% or as high as 90% of diesel exhaust particulates [12, 13].

2.2 Peritoneal macrophage collection, culture conditions, and DEPe treatment

Sixteen-week old male C57BL/6J mice were injected with thioglycollate to elicit macrophage infiltration into the peritoneal cavity [14]. Four days after thioglycollate injection, peritoneal macrophages were collected by intraperitoneal lavage, pooled, and then cultured in DMEM media containing 1% fetal bovine serum (FBS) [14]. The following day, cells were then treated with either 25 μg/mL DEPe or media-only for four hours (n=2/group). The same DEPe concentration or higher has been employed in previous in vitro studies from our group [9, 15, 16]. This DEPe concentration is estimated to be within range of what could potentially be deposited in the respiratory tract of a high-risk individual (i.e., someone who lives/works near particle sources) or even someone actively exercising outdoors [17, 18].

2.3 Affymetrix microarray profiling of DEPe-exposed peritoneal macrophages

mRNA was isolated from the peritoneal macrophages as described previously by Bennett et al. [19], and the genetic profiles were analyzed using Affymetrix HT MG-430A arrays. These arrays contained probe sets for 22,416 transcripts. Pre-processing of the microarray dataset utilized robust multi-array average (RMA) normalization. This method performs background correction, quantile normalization, and linear model fitting to the dataset [20]. The data for control cells, treated with media only, has been made available on the Gene Expression Omnibus (GEO) repository website (GEO Accession number GSE38705 [14]) as a part of another study evaluating the gene expression profiles after lipopolysaccharide

(LPS) and oxidized 1-palmitoyl-2-arachidonoyl-sn-glycero-3-phosphocholine (oxPAPC) treatments as compared with control (media-only). The data for DEPe-treated cells has not been previously reported.

2.4 In vivo DEP exposures in mice for single cell studies

Thirteen-week-old male C57BL/6J mice were instilled either with 200 μg DEP in 100 μL PBS or with 100 μL PBS only (control) via oropharyngeal aspiration (n=2/group). In this procedure, the mice were anesthetized with 5% isoflurane (with 1 L of oxygen flow) and then placed on a stand to allow access to the oral cavity. One dose of 100 uL of the treatment (PBS or DEP) was pipetted into the back of the throat, where the solution would reach the lungs upon breathing. This dosage of 200 μg DEP is within range of what has been previously used by other groups in protocols with a one-time instillation [21] or multiple instillations [22].

2.5 Lung cell isolation for single-cell RNA sequencing (scRNA-seq)

While two mice per group (DEP-treated vs. PBS-treated) were employed in the single cell analyses, hundreds of alveolar macrophage cells were obtained from each group (1,006 and 883, respectively), and analyses were done at the individual cell level, thereby offering sufficient statistical power. All lobes (superior, middle, inferior, and post-caval lobes) of the right lung of each mouse were harvested upon euthanasia for single cell dissociation. The lobes were kept in PBS on ice and then the tissue was disrupted via grinding. The tissue was transferred into a tube and then centrifuged at 300 g for ten minutes at 4°C. The supernatant was removed and then the pellet was resuspended in the dissociation media (DMEM media, containing 10% FBS, 40 mg/mL of bovine serum albumin (BSA), and 1 mg/mL of collagenase I). Collagenase I (cat. no. LS004194, Worthington Biochemical Corporation, Lakewood, NJ) was chosen based on its recommendation by the vendor for digestion of lungs. The solution was incubated at 37°C for one hour. During the hour, the tissue was pipetted gently up and down every five minutes to allow for aeration. Afterwards, the dissociated cells were passed through a 70 μm cell strainer and centrifuged at 300 g for ten minutes at 4°C [23]. The supernatant was removed, and the cell pellet was resuspended in PBS containing 2 mM EDTA. The cells were then passed through a 40 μm cell strainer and centrifuged at 300 g for ten minutes at 4°C. The supernatant was removed once more, and the cell pellet was resuspended in PBS containing 0.01% BSA. The cells were counted, and the concentration was adjusted to 1×10^5 cells/mL.

Barcoding of single cells was done using the Drop-seq protocol Version 3.1 available online (http://mccarrolllab.com/dropseq/) and described previously [24]. To generate STAMPs (single-cell transcriptomes attached to microparticles), lung cell samples were run through an aquapel-treated Drop-seq microfluidic device (FlowJEM, Toronto, Canada) where single cells were combined with droplet generation oil (Bio-Rad, Hercules, CA) and barcoded beads (ChemGenes, Wilmington, MA) in lysis buffer into droplets. After STAMPs generation, oil droplets were broken, and cDNA synthesis was performed [24]. Libraries were then prepared, using the Drop-seq protocol with some minor modifications [25]. For the PCR step, 4000 beads were used per tube and the number of cycles was changed to 4 + 11. cDNA and library quantity and quality were measured using the Agilent TapeStation

system. Paired-end sequencing was done on the Illumina HiSeq 4000 (Illumina, San Diego, CA) instrument using the Drop-seq custom read primer. Alveolar macrophages were identified from the single cell population as described in the Statistical analyses section.

2.6 Gene pathway analysis

Analysis of enriched pathways in the Affymetrix and scRNA-seq datasets was conducted using the online Gene Ontology (GO) Consortium resource [26, 27] and the Database for Annotation, Visualization and Integrated Discovery (DAVID) Bioinformatics Resources 6.8 [28]. The GO Consortium resource used PANTHER (Protein ANalysis THrough Evolutionary Relationships) tools for evaluating gene set enrichment [29, 30], and genes were mapped to pathways using the PANTHER Overrepresentation Test against the Reactome version 65 database released on 2019–03-12. Reactome pathways are ordered in a hierarchical fashion [31], with parental (top-level) pathways followed by child (sub-level) pathways. With the DAVID Bioinformatics Resources, analysis of gene set enrichment was performed to map genes to BioCarta and Kyoto Encyclopedia of Genes and Genomes (KEGG) pathways.

2.7 Statistical analyses

The analysis of differential gene expression in the Affymetrix microarrays was performed using the limma package in R. The limma package performs linear modeling of the microarray data to determine differentially expressed genes between different conditions [32]. The reported significance values were adjusted for multiple testing using the Benjamini & Hochberg correction, which controls the false discovery rate (FDR), and thus an FDR < 0.05 was considered statistically significant [32].

Clustering of the cells that were identified through scRNA-seq was done using the Seurat package in R [33]. This package utilizes t-distributed stochastic neighbor embedding (t-SNE) to calculate distances between the transcriptomes of cells and map them into spatial patterns [24, 34, 35]. The Immunological Genome Project resource [36] and the Mouse Cell Atlas [37] were used for classifying cells into their likely cell types. Differentially expressed genes (DEGs) were identified using the Wilcoxon rank-sum test in the Seurat package in R, with FDR < 0.05 considered as statistically significant [33].

Reactome, BioCarta, and KEGG pathways enrichment was assessed using Fisher’s exact test with FDR correction for multiple testing. Pathways with FDR < 0.05 were considered statistically significant.

3. Results

3.1 In vitro DEPe treatment promoted antioxidant responses in peritoneal macrophages

To analyze the effects of DEPe in vitro, peritoneal macrophages were harvested from C57BL/6J mice and treated with either DEPe or media-only for four hours. Their gene expression profile was analyzed with Affymetrix arrays. Expression of 12,976 unique genes was detected from 22,416 transcripts that were covered by the microarrays. Differential gene expression analysis revealed that 749 genes were significantly dysregulated by DEPe

treatment as compared to media-only (FDR < 0.05). Approximately half of the genes were upregulated while the other half were downregulated (Figure 1). Several antioxidant enzymes were among the most highly upregulated differentially expressed genes (DEGs). In fact, five antioxidant genes were among the top ten DEGs (Table 1). The antioxidant enzyme heme oxygenase 1 (*Hmox1*), responsible for catabolism of heme groups, was not only the most significant DEG but also the fourth most upregulated gene in terms of fold change (Table 1). The other antioxidant genes included glutamate-cysteine ligase, modifier subunit (*Gclm*); sulfiredoxin 1 homolog (*Srxn1*); glutamate-cysteine ligase, catalytic subunit (*Gclc*); and thioredoxin reductase 1 (*Txnrd1*) (Table 1).

Pathway analyses indicated that the 749 DEGs were enriched in multiple pathways. The top five Reactome parental pathways were metabolism, immune system, transport of small molecules, hemostasis, and cellular responses to external stimuli, with several child (sub-level) pathways within each parental pathway (Figure 2A). KEGG pathway analysis also revealed pathways related to immune responses, metabolism, and antioxidant responses, such as the chemokine signaling pathway, central carbon metabolism in cancer, and glutathione metabolism, respectively, among several others (Table 2). Interestingly, immunological pathways included those involved in both innate immune system as well as adaptive immune system (Figure 2). When circumscribing pathway analyses to the 379 upregulated genes, Reactome pathways related to metabolism, the immune system, and transport of small molecules remained in the top three (Figure 2B). BioCarta and KEGG analyses identified three pathways, including pathways involved in glutathione metabolism and oxidative stress-induced gene expression via Nrf2 (nuclear factor, erythroid derived 2, like 2) (Table 3). These pathways (Table 3) and antioxidant DEGs (Table 1) suggested that DEPe induced significant oxidative stress in peritoneal macrophages, likely due to its high content in redox active chemicals, followed by a strong antioxidant response. In addition, several antioxidant genes were part of various pathways. For instance, the most significant DEG, *Hmox1*, was found not only in the metabolism and the transport of small molecules pathways (Figure 2), but also in the HIF-1 (hypoxia-inducible factor 1) signaling (Table 2) and the oxidative stress-induced gene expression via Nrf2 pathways as well (Table 3). *Txnrd1*, which was the ninth top DEG, was classified in both the detoxification of reactive oxygen species and the TP53 regulates metabolic genes pathways (Figure 2). Furthermore, *Gclm* and *Gclc* were both found in the KEGG glutathione metabolism pathway.

3.2 In vivo DEP exposure led to heterogeneous responses in alveolar macrophages

To characterize the gene expression profile elicited in alveolar macrophages by an oropharyngeal aspiration of DEP, the lungs from mice treated with DEP vs. PBS were taken for scRNA-seq analysis. Altogether, there were 1,889 alveolar macrophages that were captured in the Drop-seq protocol, comprising 1,006 from the DEP-treated group and 883 from the PBS-treated group. The cells from these groups were clustered using the Seurat package in R (Figure 3). There were 17,655 transcripts covered by the scRNA-seq platform. We detected the expression of 11,784 genes in the alveolar macrophages from the PBS-treated group and 11,827 genes in the DEP-treated group. There were 109 genes that were significantly differentially expressed between the DEP- and PBS-treated groups; 19 genes

were upregulated while 90 genes were downregulated. The top 40 DEGs are listed in Table 4.

It was noticeable that for many genes, the level of fold change among all cells was mainly achieved via increased number of cells expressing those genes as opposed to increases in the actual level of expression in individual cells, as this can be seen in the cellular expressions of some of the top DEGs (Figure 4). For instance, the S100 calcium binding protein A8 (calgranulin A) (*S100a8*) gene was downregulated by DEP treatment. There were far fewer *S100a8*-expressing DEP-treated cells than PBS-treated cells within a similar range of normalized expression levels. In addition, over 97% of the DEP-treated and over 67% of the PBS-treated alveolar macrophages showed "zero" values for *S100a8* expression (Figure 4). A similar scenario was found with S100 calcium binding protein A9 (*S100a9*), and with chitinase-like 3 (*Chi313*), which were also downregulated by DEP (Figure 4). The "zero" expression values exhibited by many cells for these genes (Figure 4) could be due to dropouts from the methodology rather than true lack of expression, which is well known to scRNA-seq technology [38]. On the other hand, for *mt-Rnr2* expression, 100% of the DEP-treated and over 99% of the PBS-treated cells demonstrated expression of this gene (Figure 4). Thus, the fold change difference in this case (DEP-induced upregulation) reflected DEP-induced increases in the actual level of expression in each cell as opposed to only differences in the numbers of expressing cells.

Similar to the Affymetrix data, immunological pathways were prominently dysregulated in alveolar macrophages from mice exposed to DEP, especially from the innate immune system (Figure 5). Some of the genes involved in these immune pathways included acetyl-coenzyme A acyltransferase 1B (*Acaa1b*); ATPase, H+ transporting, lysosomal V0 subunit D2 (*Atp6v0d2*); CD36 molecule (*Cd36*); CD74 antigen (invariant polypeptide of major histocompatibility complex, class II antigen-associated) (*Cd74*); cystatin B (*Cstb*); histocompatibility 2, class II antigen A, alpha (*H2-Aa*); and tumor necrosis factor (*Tnf*) (Figure 6). It is worth noting that despite all these immune-related genes being significantly upregulated with DEP exposure, there was marked heterogeneity at the cellular level. For example, macrophages harvested from DEP-treated mice exhibited a significant upregulation in *Acaa1b* (Figure 6), but in spite of this, only 73.1% of cells expressed higher levels than the average expression level of cells harvested from control mice, while 26.9% of cells (including those with zero values) had expression levels even lower than the average of the controls. Similar effects were observed with other genes as illustrated by the expression plots for *Cd36*, *Cstb*, and *Tnf* (Figure 6). Interestingly, among the thousands of genes that were analyzed using Affymetrix and scRNA-seq, only six genes were actually commonly dysregulated in the same direction in both technologies (Table 5 and Figure 7); three were upregulated, while the other three were downregulated.

4. Discussion

Our studies demonstrate that macrophages exhibited strong and wide-ranging responses to air pollutants, affecting a multiplicity of molecular pathways especially involved in innate immunity and antioxidant defense. We analyzed the genome-wide responses of macrophages to DEP in both in vitro and in vivo conditions, using Affymetrix microarray and scRNA-seq

technologies, respectively. The mRNA expressions of genes involved in immune-related pathways were prominently dysregulated in both conditions while antioxidant responses were predominant only in vitro. Additionally, the analyses of single cell expression data allowed us to identify a marked heterogeneity in individual cell responses.

Previous studies have shown that myeloid cells such as macrophages exhibit robust responses to air pollution. Thus, PM_{10} (PM < 10 μm in diameter) and DEP exposures have been reported to lead to infiltration of macrophages in the lung alveoli [39–41] where these cells can phagocytose foreign particles [42–45], and have significant involvement in inflammatory diseases associated with air pollution exposure such as asthma and chronic obstructive pulmonary disease (COPD) [46]. Indeed, inflammatory processes were significantly dysregulated in our alveolar and peritoneal macrophages from mice exposed to DEP or DEP chemicals, respectively.

In the in vitro study, we used DEPe, which has been well characterized, amply used as a model pollutant, and suitable for tissue culture studies [9, 15, 18]. Peritoneal macrophages treated with DEPe exhibited significant enrichment of immunological pathways. Thus, the same pathways under the immune system Reactome pathway group (innate immune system and neutrophil degranulation) were dysregulated in both peritoneal (Figure 2) and alveolar macrophages (Figure 5) but the individual genes that were differentially expressed were different. In fact, only one gene among these immune pathways, *Cd36*, was differentially expressed in the same direction (upregulated with air pollutant treatment) in both Affymetrix and scRNA-seq datasets (Table 5). There were two other immune system genes in common (*Ctsc* and *Hsp90aa1*) that were dysregulated, however the dysregulations were in opposite directions (Table 5). This was remarkable considering that the *Mus musculus* reference lists used in the Reactome analysis (Reactome version 65 database released on 2019–03-12) included >1,700 genes in the immune system pathway, >1,000 genes in the innate immune system pathway, and >500 genes in the neutrophil degranulation pathway. Interestingly, neutrophil degranulation was a significantly affected pathway among macrophages in both experiments (Figure 2 & 5). Under in vitro conditions, it is possible that peritoneal macrophages harvested four days after the administration of thioglycollate could contain a small number of neutrophils. Alternatively, activation of macrophages could lead to neutrophil migration and degranulation [47]. Indeed, enrichment of the same pathway in vivo appears to support this latter possibility, although there could have been cellular misclassification in the analyses of scRNA transcripts as well.

We observed a marked upregulation of antioxidant genes in DEPe-treated peritoneal macrophages, as five out of the top ten upregulated genes were antioxidants – *Hmox1*, *Gclm*, *Srxn1*, *Gclc*, and *Txnrd1* (Table 1), all regulated by the NRF2 transcription factor. In fact, the significantly enriched pathways identified from the Affymetrix data included oxidative stress-induced gene expression via Nrf2 pathway (BioCarta) (Table 3) as well as Reactome pathways involved in cellular responses to stress and in detoxification of reactive oxygen species (Figure 2). This is consistent with previous studies where rat alveolar macrophages exposed to DEPe showed increased expression of *Hmox1*, *Hmox2*, peroxiredoxin 1 (*Prdx1*), NAD(P)H quinone dehydrogenase 1 (*Nqo1*), and a subunit of glutathione S-transferase (*Gstp1*) [48]. In addition, DEPe treatment of RAW 264.7

macrophages and THP-1 monocytes led to a reduction in the ratio of reduced glutathione to oxidized glutathione (GSH/GSSG), indicative of increased oxidative stress [10, 49].

Oxidative stress responses, however, were not apparent in the in vivo study. Indeed, none of the antioxidant genes that were upregulated under in vitro conditions were dysregulated in alveolar macrophages harvested from DEP-exposed mice. This was surprising since inflammatory responses elicited by air pollutant exposures are thought to develop after induction of oxidative stress. In addition, various transcription factors can regulate the expression of inflammatory molecules in a prooxidative environment [50]. For example, mice lacking the NRF2 transcription factor, considered to be a master regulator of antioxidant defense and phase II detoxifying enzymes, have been shown to be more susceptible to toxins, like developing an asthma-like condition after DEP inhalation [51] or developing emphysema after cigarette smoke exposures [52, 53]. Differences in the type of DEP used (whole DEP in vivo vs. DEPe in vitro) or the type of macrophages studied (alveolar vs. peritoneal) are unlikely to explain the lack of antioxidant responses in live mice. Indeed, intratracheal administration of DEP in mice has been reported to induce *Hmox1* expression and oxidative DNA damage in the lungs, 1 hour and 22 hours after the DEP administration [54]. This is consistent with a human study where DEP exposure for two hours led to increased oxidized glutathione in the bronchoalveolar lavage fluid, 18 hours post-exposure [55]. Although the duration of exposures in our study were similar in both approaches (five hours in vivo and four hours in vitro), it is possible that the kinetics for antioxidant responses vary between cells in culture vs. those in live exposures.

There were other significant differences in the expression profiles observed in the in vitro and in vivo studies. Indeed, only eleven genes were commonly dysregulated in the Affymetrix and scRNA-seq data (Table 5), with just six of those genes being dysregulated in the same direction in both conditions (Figure 7). These differences in responses could be due to the type or concentrations of DEP used. Whole particles were administered to live mice to mimic “real-world” exposures, but an organic extract of the particles (DEPe), highly enriched in the organic components of DEP and with a large amount of redox active chemicals [10], was used under cell culture conditions, given its solubility in media. The differences could also have been due to the two types of macrophage populations, alveolar macrophages in the live exposures vs. peritoneal macrophages in the vitro treatments. Indeed, different macrophage populations exhibit large phenotypic differences in response to the same stimuli. For instance, alveolar macrophages from several mouse strains were demonstrated to have less ability to clear apoptotic T cells than peritoneal macrophages under both in vitro and in vivo conditions [56].

The single cell analyses of RNA-seq allowed us to identify a marked heterogeneity in the population of individual cells isolated by the Drop-seq protocol, which would have been otherwise impossible to determine with microarray technology. While there were dozens of genes that were, on average, significantly different between DEP and control PBS treatments, there were marked differences in the mRNA expression of DEP-dysregulated genes among the individual cells (inter-cell heterogeneity). Thus, several immune-related genes were significantly upregulated in the DEP-treated vs. PBS-treated cells, which included *Acaa1b*, *Atp6v0d2*, *Cd36*, *Cd74*, *Cstb*, *H2-Aa*, and *Tnf* (Figure 6). But the

upregulation of these genes varied a lot among the individual cells harvested from DEP-treated mice. In addition, not all of these genes were upregulated in the same cells. For example, DEP upregulated the expression of *Cd74*, *Cstb*, *H2-Aa*, and *Tnf* in a subset of cells that actually exhibited low expression of *Acaa1b*, *Atp6v0d2*, and *Cd36* instead (boxed regions in Figure 6), even though all seven genes were upregulated by DEP overall. Thus, there was not only inter-cell heterogeneity of gene expression across different alveolar macrophages but also intra-cell heterogeneity of gene expression patterns exhibited by those alveolar macrophages. The use of scRNA-seq has allowed other groups to identify significant cell heterogeneity in a subpopulation of amacrine neurons in the retina [24], in tanycyte cells in the hypothalamus [57], and in macrophages and monocyte-derived dendritic cells in mouse aortic atherosclerotic lesions [58], with the identification of new cell populations with specific gene expression signatures suggesting specialized functions [57, 58]. In our study, the large heterogeneities that we observed could be due to the different degrees in which macrophages from various parts of the lungs were actually exposed to the DEP. Indeed, particles do not disperse evenly over the whole lungs upon instillation, thereby causing some macrophages to come into close contact with the particles to phagocytose them, while causing other macrophages to be untouched by the particles.

A limitation of our study is that while both in vitro and in vivo experiments allowed us to identify multiple immunological pathways that were dysregulated by DEP, they were relatively broad. Although they could mediate development of cardiovascular diseases, they could also be involved in the development of many other disorders where the immune system is important, such as allergies and pulmonary diseases, among several others. In addition, pathway analyses were exclusively based on mRNA expression data. Evaluation of expression at the protein level would be informative similar to how other studies have employed immunostaining to validate their scRNA-seq data [37, 57, 59], which will be the focus of future studies.

5. Conclusions

Our studies indicate that macrophages exhibit robust responses against diesel exhaust particulate pollutants. Under cell culture conditions, antioxidant and immune molecular pathways were prominent in peritoneal macrophages treated with DEPe. In alveolar macrophages from mice exposed to DEP via oropharyngeal aspiration, immune responses were strongly evoked as well. These studies utilized two different technologies, Affymetrix microarrays and scRNA-seq. While previous studies have used microarrays to analyze genome-wide changes to air pollutants [48, 60], this is the first report using scRNA-seq to elucidate changes induced by air pollution at the cellular level. The scRNA-seq platform allowed us to identify marked heterogeneity in genes and pathways that are activated within each cell that would not have been possible with the microarray platform. Altogether, DEP pollutants elicited inflammatory pathways in macrophages that may mediate the development of pulmonary and systemic vascular effects.

Acknowledgements

We are grateful to Andrew Saxon who generously provided the DEP.

Funding Sources

This work was supported by the National Institutes of Health: National Institute of Environmental Health Sciences (ONES RO1 Award ES016959 and R01 ES029395 to JAA, as well as the Training Grant in Molecular Toxicology T32 ES015457 to MB and GD), and the National Heart, Lung, and Blood Institute (R01 HL28581 to AJL).

Abbreviations

DEG	differentially expressed gene
DEP	diesel exhaust particles
DEPe	diesel exhaust particles extract
FDR	false discovery rate
HMOX1	heme oxygenase 1
NRF2	nuclear factor, erythroid derived 2, like 2
PM	particulate matter
ROS	reactive oxygen species
scRNA-seq	single-cell RNA sequencing

References

[1]. Brook RD, Rajagopalan S, Pope CA 3rd, Brook JR, Bhatnagar A, Diez-Roux AV, Holguin F, Hong Y, Luepker RV, Mittleman MA, Peters A, Siscovick D, Smith SC Jr., Whitsel L, Kaufman JD, Particulate matter air pollution and cardiovascular disease: An update to the scientific statement from the American Heart Association, Circulation 121(21) (2010) 2331–78. [PubMed: 20458016]

[2]. National Toxicology Program, Report on Carcinogens, U.S. Department of Health and Human Services, Public Health Service, Research Triangle Park, NC, 2016.

[3]. Shirmohammadi F, Wang D, Hasheminassab S, Verma V, Schauer JJ, C. Sioutas SMM, Oxidative potential of on-road fine particulate matter (PM2.5) measured on major freeways of Los Angeles, CA, and a 10-year comparison with earlier roadside studies, Atmospheric Environment 148 (2017) 102–114.

[4]. U.S. Environmental Protection Agency, NAAQS Table. https://www.epa.gov/criteria-air-pollutants/naaqs-table. (Accessed August 13 2019).

[5]. Pope CA 3rd, Burnett RT, Thurston GD, Thun MJ, Calle EE, Krewski D, Godleski JJ, Cardiovascular mortality and long-term exposure to particulate air pollution: epidemiological evidence of general pathophysiological pathways of disease, Circulation 109(1) (2004) 71–7. [PubMed: 14676145]

[6]. Araujo JA, Barajas B, Kleinman M, Wang X, Bennett BJ, Gong KW, Navab M, Harkema J, Sioutas C, Lusis AJ, Nel AE, Ambient particulate pollutants in the ultrafine range promote early atherosclerosis and systemic oxidative stress, Circ Res 102(5) (2008) 589–96. [PubMed: 18202315]

[7]. Araujo JA, Nel AE, Particulate matter and atherosclerosis: role of particle size, composition and oxidative stress, Particle and fibre toxicology 6 (2009) 24. [PubMed: 19761620]

[8]. Fiordelisi A, Piscitelli P, Trimarco B, Coscioni E, Iaccarino G, Sorriento D, The mechanisms of air pollution and particulate matter in cardiovascular diseases, Heart failure reviews 22(3) (2017) 337–347. [PubMed: 28303426]

[9]. Yin F, Ramanathan G, Zhang M, Araujo JA, Prooxidative effects of ambient pollutant chemicals are inhibited by HDL, Journal of biochemical and molecular toxicology 27(2) (2013) 172–83. [PubMed: 23420698]

[10]. Li N, Wang M, Oberley TD, Sempf JM, Nel AE, Comparison of the pro-oxidative and proinflammatory effects of organic diesel exhaust particle chemicals in bronchial epithelial cells and macrophages, J Immunol 169(8) (2002) 4531–41. [PubMed: 12370390]

[11]. Yin F, Lawal A, Ricks J, Fox JR, Larson T, Navab M, Fogelman AM, Rosenfeld ME, Araujo JA, Diesel exhaust induces systemic lipid peroxidation and development of dysfunctional pro-oxidant and pro-inflammatory high-density lipoprotein, Arteriosclerosis, thrombosis, and vascular biology 33(6) (2013) 1153–61.

[12]. Williams DJ, Milne JW, Quigley SM, Roberts DB, Kimberlee MC, Particulate emissions from 'in-use' motor vehicles - II. Diesel vehicles, Atmospheric Environment 23(12) (1989) 15.

[13]. National Toxicology Program, Diesel Exhaust Particulates, Report on Carcinogens, U.S. Department of Health and Human Services, 2011, pp. 153–156.

[14]. Orozco LD, Bennett BJ, Farber CR, Ghazalpour A, Pan C, Che N, Wen P, Qi HX, Mutukulu A, Siemers N, Neuhaus I, Yordanova R, Gargalovic P, Pellegrini M, Kirchgessner T, Lusis AJ, Unraveling inflammatory responses using systems genetics and geneenvironment interactions in macrophages, Cell 151(3) (2012) 658–70. [PubMed: 23101632]

[15]. Lawal A, Zhang M, Dittmar M, Lulla A, Araujo JA, Heme oxygenase-1 protects endothelial cells from the toxicity of air pollutant chemicals, Toxicology and applied pharmacology 284(3) (2015) 281–291. [PubMed: 25620054]

[16]. Yin F, Gupta R, Vergnes L, Driscoll WS, Ricks J, Ramanathan G, Stewart JA, Shih DM, Faull KF, Beaven SW, Lusis AJ, Reue K, Rosenfeld ME, Araujo JA, Diesel Exhaust Induces Mitochondrial Dysfunction, Hyperlipidemia, and Liver Steatosis, Arteriosclerosis, thrombosis, and vascular biology 39(9) (2019) 1776–1786.

[17]. Phalen RF, Oldham MJ, Nel AE, Tracheobronchial particle dose considerations for in vitro toxicology studies, Toxicol Sci 92(1) (2006) 126–32. [PubMed: 16597657]

[18]. Gong KW, Zhao W, Li N, Barajas B, Kleinman M, Sioutas C, Horvath S, Lusis AJ, Nel A, Araujo JA, Air-pollutant chemicals and oxidized lipids exhibit genome-wide synergistic effects on endothelial cells, Genome biology 8(7) (2007) R149.

[19]. Bennett BJ, Farber CR, Orozco L, Kang HM, Ghazalpour A, Siemers N, Neubauer M, Neuhaus I, Yordanova R, Guan B, Truong A, Yang WP, He A, Kayne P, Gargalovic P, Kirchgessner T, Pan C, Castellani LW, Kostem E, Furlotte N, Drake TA, Eskin E, Lusis AJ, A high-resolution association mapping panel for the dissection of complex traits in mice, Genome research 20(2) (2010) 281–90. [PubMed: 20054062]

[20]. Irizarry RA, Hobbs B, Collin F, Beazer-Barclay YD, Antonellis KJ, Scherf U, Speed TP, Exploration, normalization, and summaries of high density oligonucleotide array probe level data, Biostatistics (Oxford, England) 4(2) (2003) 249–64.

[21]. Nagashima M, Kasai H, Yokota J, Nagamachi Y, Ichinose T, Sagai M, Formation of an oxidative DNA damage, 8-hydroxydeoxyguanosine, in mouse lung DNA after intratracheal instillation of diesel exhaust particles and effects of high dietary fat and beta-carotene on this process, Carcinogenesis 16(6) (1995) 1441–5. [PubMed: 7540513]

[22]. Sagai M, Furuyama A, Ichinose T, Biological effects of diesel exhaust particles (DEP). III. Pathogenesis of asthma like symptoms in mice, Free radical biology & medicine 21(2) (1996) 199–209. [PubMed: 8818635]

[23]. Alphonse RS, Vadivel A, Zhong S, McConaghy S, Ohls R, Yoder MC, Thebaud B, The isolation and culture of endothelial colony-forming cells from human and rat lungs, Nature protocols 10(11) (2015) 1697–708. [PubMed: 26448359]

[24]. Macosko EZ, Basu A, Satija R, Nemesh J, Shekhar K, Goldman M, Tirosh I, Bialas AR, Kamitaki N, Martersteck EM, Trombetta JJ, Weitz DA, Sanes JR, Shalek AK, Regev A, McCarroll SA, Highly Parallel Genome-wide Expression Profiling of Individual Cells Using Nanoliter Droplets, Cell 161(5) (2015) 1202–1214. [PubMed: 26000488]

[25]. Arneson D, Zhang G, Ying Z, Zhuang Y, Byun HR, Ahn IS, Gomez-Pinilla F, Yang X, Single cell molecular alterations reveal target cells and pathways of concussive brain injury, Nat Commun 9(1) (2018) 3894. [PubMed: 30254269]

[26]. Ashburner M, Ball CA, Blake JA, Botstein D, Butler H, Cherry JM, Davis AP, Dolinski K, Dwight SS, Eppig JT, Harris MA, Hill DP, Issel-Tarver L, Kasarskis A, Lewis S, Matese JC, Richardson JE, Ringwald M, Rubin GM, Sherlock G, Gene ontology: tool for the unification of biology. The Gene Ontology Consortium, Nature genetics 25(1) (2000) 25–9. [PubMed: 10802651]

[27]. The Gene Ontology Resource: 20 years and still GOing strong, Nucleic Acids Res 47(D1) (2019) D330–d338. [PubMed: 30395331]

[28]. Huang DW, Sherman BT, Lempicki RA, Systematic and integrative analysis of large gene lists using DAVID bioinformatics resources, Nature protocols 4(1) (2009) 44–57. [PubMed: 19131956]

[29]. The Gene Ontology Consortium, Expansion of the Gene Ontology knowledgebase and resources, Nucleic acids research 45(D1) (2017) D331–d338. [PubMed: 27899567]

[30]. Mi H, Muruganujan A, Ebert D, Huang X, Thomas PD, PANTHER version 14: more genomes, a new PANTHER GO-slim and improvements in enrichment analysis tools, Nucleic Acids Res 47(D1) (2019) D419–d426. [PubMed: 30407594]

[31]. Croft D, O'Kelly G, Wu G, Haw R, Gillespie M, Matthews L, Caudy M, Garapati P, Gopinath G, Jassal B, Jupe S, Kalatskaya I, Mahajan S, May B, Ndegwa N, Schmidt E, Shamovsky V, Yung C, Birney E, Hermjakob H, D'Eustachio P, Stein L, Reactome: a database of reactions, pathways and biological processes, Nucleic Acids Res 39(Database issue) (2011) D691–7. [PubMed: 21067998]

[32]. Smyth GK, Ritchie M, Thorne N, Wettenhall J, Shi W, Hu Y, limma: Linear Models for Microarray and RNA-Seq Data: User's Guide, The Walter and Eliza Hall Institute of Medical Research, Melbourne, Australia, 2018.

[33]. Butler A, Hoffman P, Smibert P, Papalexi E, Satija R, Integrating single-cell transcriptomic data across different conditions, technologies, and species, Nature biotechnology 36(5) (2018) 411–420.

[34]. Satija R, Farrell JA, Gennert D, Schier AF, Regev A, Spatial reconstruction of single-cell gene expression data, Nature biotechnology 33(5) (2015) 495–502.

[35]. van der Maaten L, Hinton G, Visualizing Data using t-SNE, Journal of Machine Learning Research 9 (2008) 2579–2605.

[36]. Heng TS, Painter MW, The Immunological Genome Project: networks of gene expression in immune cells, Nature immunology 9(10) (2008) 1091–4. [PubMed: 18800157]

[37]. Han X, Wang R, Zhou Y, Fei L, Sun H, Lai S, Saadatpour A, Zhou Z, Chen H, Ye F, Huang D, Xu Y, Huang W, Jiang M, Jiang X, Mao J, Chen Y, Lu C, Xie J, Fang Q, Wang Y, Yue R, Li T, Huang H, Orkin SH, Yuan GC, Chen M, Guo G, Mapping the Mouse Cell Atlas by Microwell-Seq, Cell 172(5) (2018) 1091–1107.e17.

[38]. Hwang B, Lee JH, Bang D, Single-cell RNA sequencing technologies and bioinformatics pipelines, Exp Mol Med 50(8) (2018) 96.

[39]. Yanamala N, Hatfield MK, Farcas MT, Schwegler-Berry D, Hummer JA, Shurin MR, Birch ME, Gutkin DW, Kisin E, Kagan VE, Bugarski AD, Shvedova AA, Biodiesel versus diesel exposure: enhanced pulmonary inflammation, oxidative stress, and differential morphological changes in the mouse lung, Toxicology and applied pharmacology 272(2) (2013) 373–83. [PubMed: 23886933]

[40]. Farina F, Sancini G, Battaglia C, Tinaglia V, Mantecca P, Camatini M, Palestini P, Milano summer particulate matter (PM10) triggers lung inflammation and extra pulmonary adverse events in mice, PloS one 8(2) (2013) e56636.

[41]. Rizzo AM, Corsetto PA, Farina F, Montorfano G, Pani G, Battaglia C, Sancini G, Palestini P, Repeated intratracheal instillation of PM10 induces lipid reshaping in lung parenchyma and in extra-pulmonary tissues, PloS one 9(9) (2014) e106855.

[42]. Kulkarni N, Pierse N, Rushton L, Grigg J, Carbon in airway macrophages and lung function in children, N Engl J Med 355(1) (2006) 21–30. [PubMed: 16822993]

[43]. Finch GL, Hobbs CH, Blair LF, Barr EB, Hahn FF, Jaramillo RJ, Kubatko JE, March TH, White RK, Krone JR, Menache MG, Nikula KJ, Mauderly JL, Van Gerpen J, Merceica MD, Zielinska B, Stankowski L, Burling K, Howell S, Effects of subchronic inhalation exposure of rats to emissions from a diesel engine burning soybean oil-derived biodiesel fuel, Inhal Toxicol 14(10) (2002) 1017–48. [PubMed: 12396409]

[44]. Strom KA, Garg BD, Johnson JT, D'Arcy JB, Smiler KL, Inhaled particle retention in rats receiving low exposures of diesel exhaust, Journal of toxicology and environmental health 29(4) (1990) 377–98. [PubMed: 1691304]

[45]. Suwa T, Hogg JC, Quinlan KB, Ohgami A, Vincent R, van Eeden SF, Particulate air pollution induces progression of atherosclerosis, Journal of the American College of Cardiology 39(6) (2002) 935–42. [PubMed: 11897432]

[46]. Becker S, Soukup JM, Gallagher JE, Differential particulate air pollution induced oxidant stress in human granulocytes, monocytes and alveolar macrophages, Toxicology in vitro : an international journal published in association with BIBRA 16(3) (2002) 209–18. [PubMed: 12020593]

[47]. Gomez-Cambronero J, Horn J, Paul CC, Baumann MA, Granulocyte-macrophage colony-stimulating factor is a chemoattractant cytokine for human neutrophils: involvement of the ribosomal p70 S6 kinase signaling pathway, J Immunol 171(12) (2003) 6846–55. [PubMed: 14662891]

[48]. Koike E, Hirano S, Shimojo N, Kobayashi T, cDNA microarray analysis of gene expression in rat alveolar macrophages in response to organic extract of diesel exhaust particles, Toxicol Sci 67(2) (2002) 241–6. [PubMed: 12011483]

[49]. Li N, Kim S, Wang M, Froines J, Sioutas C, Nel A, Use of a stratified oxidative stress model to study the biological effects of ambient concentrated and diesel exhaust particulate matter, Inhal Toxicol 14(5) (2002) 459–86. [PubMed: 12028803]

[50]. Wilson JN, Pierce JD, Clancy RL, Reactive oxygen species in acute respiratory distress syndrome, Heart & lung : the journal of critical care 30(5) (2001) 370–5. [PubMed: 11604979]

[51]. Li YJ, Takizawa H, Azuma A, Kohyama T, Yamauchi Y, Takahashi S, Yamamoto M, Kawada T, Kudoh S, Sugawara I, Disruption of Nrf2 enhances susceptibility to airway inflammatory responses induced by low-dose diesel exhaust particles in mice, Clinical immunology (Orlando, Fla.) 128(3) (2008) 366–73.

[52]. Rangasamy T, Cho CY, Thimmulappa RK, Zhen L, Srisuma SS, Kensler TW, Yamamoto M, Petrache I, Tuder RM, Biswal S, Genetic ablation of Nrf2 enhances susceptibility to cigarette smoke-induced emphysema in mice, The Journal of clinical investigation 114(9) (2004) 1248–59. [PubMed: 15520857]

[53]. Sussan TE, Rangasamy T, Blake DJ, Malhotra D, El-Haddad H, Bedja D, Yates MS, Kombairaju P, Yamamoto M, Liby KT, Sporn MB, Gabrielson KL, Champion HC, Tuder RM, Kensler TW, Biswal S, Targeting Nrf2 with the triterpenoid CDDO-imidazolide attenuates cigarette smoke-induced emphysema and cardiac dysfunction in mice, Proc Natl Acad Sci U S A 106(1) (2009) 250–5. [PubMed: 19104057]

[54]. Risom L, Dybdahl M, Bornholdt J, Vogel U, Wallin H, Moller P, Loft S, Oxidative DNA damage and defence gene expression in the mouse lung after short-term exposure to diesel exhaust particles by inhalation, Carcinogenesis 24(11) (2003) 1847–52. [PubMed: 12919962]

[55]. Behndig AF, Mudway IS, Brown JL, Stenfors N, Helleday R, Duggan ST, Wilson SJ, Boman C, Cassee FR, Frew AJ, Kelly FJ, Sandstrom T, Blomberg A, Airway antioxidant and inflammatory responses to diesel exhaust exposure in healthy humans, Eur Respir J 27(2) (2006) 359–65. [PubMed: 16452593]

[56]. Hu B, Sonstein J, Christensen PJ, Punturieri A, Curtis JL, Deficient in vitro and in vivo phagocytosis of apoptotic T cells by resident murine alveolar macrophages, J Immunol 165(4) (2000) 2124–33. [PubMed: 10925298]

[57]. Chen R, Wu X, Jiang L, Zhang Y, Single-Cell RNA-Seq Reveals Hypothalamic Cell Diversity, Cell Rep 18(13) (2017) 3227–3241. [PubMed: 28355573]

[58]. Cochain C, Vafadarnejad E, Arampatzi P, Pelisek J, Winkels H, Ley K, Wolf D, Saliba AE, Zernecke A, Single-Cell RNA-Seq Reveals the Transcriptional Landscape and Heterogeneity of

Aortic Macrophages in Murine Atherosclerosis, Circ Res 122(12) (2018) 1661–1674. [PubMed: 29545365]

[59]. Grun D, Lyubimova A, Kester L, Wiebrands K, Basak O, Sasaki N, Clevers H, van Oudenaarden A, Single-cell messenger RNA sequencing reveals rare intestinal cell types, Nature 525(7568) (2015) 251–5. [PubMed: 26287467]

[60]. van Leeuwen DM, van Herwijnen MH, Pedersen M, Knudsen LE, Kirsch-Volders M, Sram RJ, Staal YC, Bajak E, van Delft JH, Kleinjans JC, Genome-wide differential gene expression in children exposed to air pollution in the Czech Republic, Mutat Res 600(1–2) (2006) 12–22. [PubMed: 16814814]

Highlights

- DEP exposure dysregulated immune responses in macrophages in vitro and in vivo.
- Under in vitro conditions, DEP induced antioxidant responses in peritoneal macrophages.
- Single-cell RNA analysis revealed marked heterogeneity among alveolar macrophage responses in vivo.

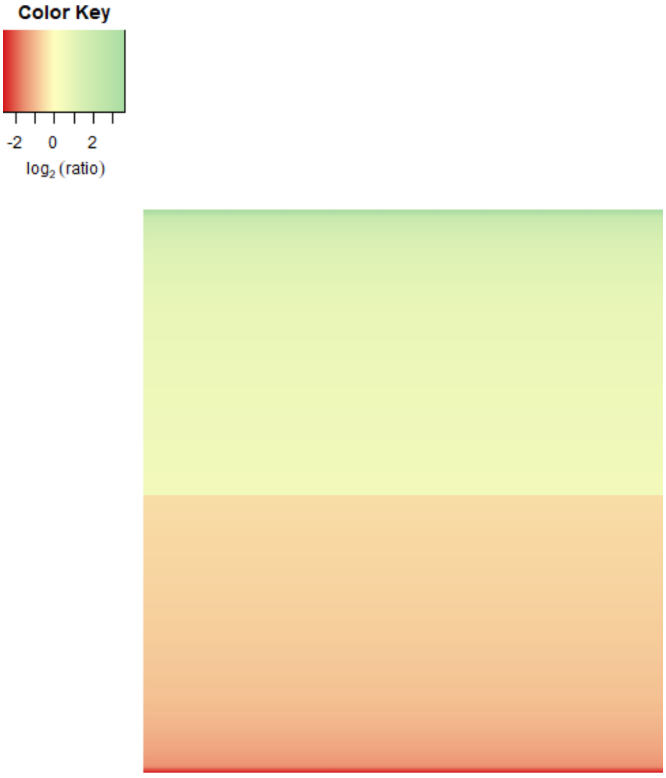

Figure 1: Dysregulated genes by DEPe.

Heat map of peritoneal macrophage expression levels in DEPe-treated over control cells, based on Affymetrix data. The genes are listed on the y-axis in decreasing order of fold change (ratio of the mRNA expression in DEPe-treated cells over controls). There were 749 genes that were differentially expressed, and the number of significantly upregulated (379) vs. significantly downregulated (370) genes was nearly equal.

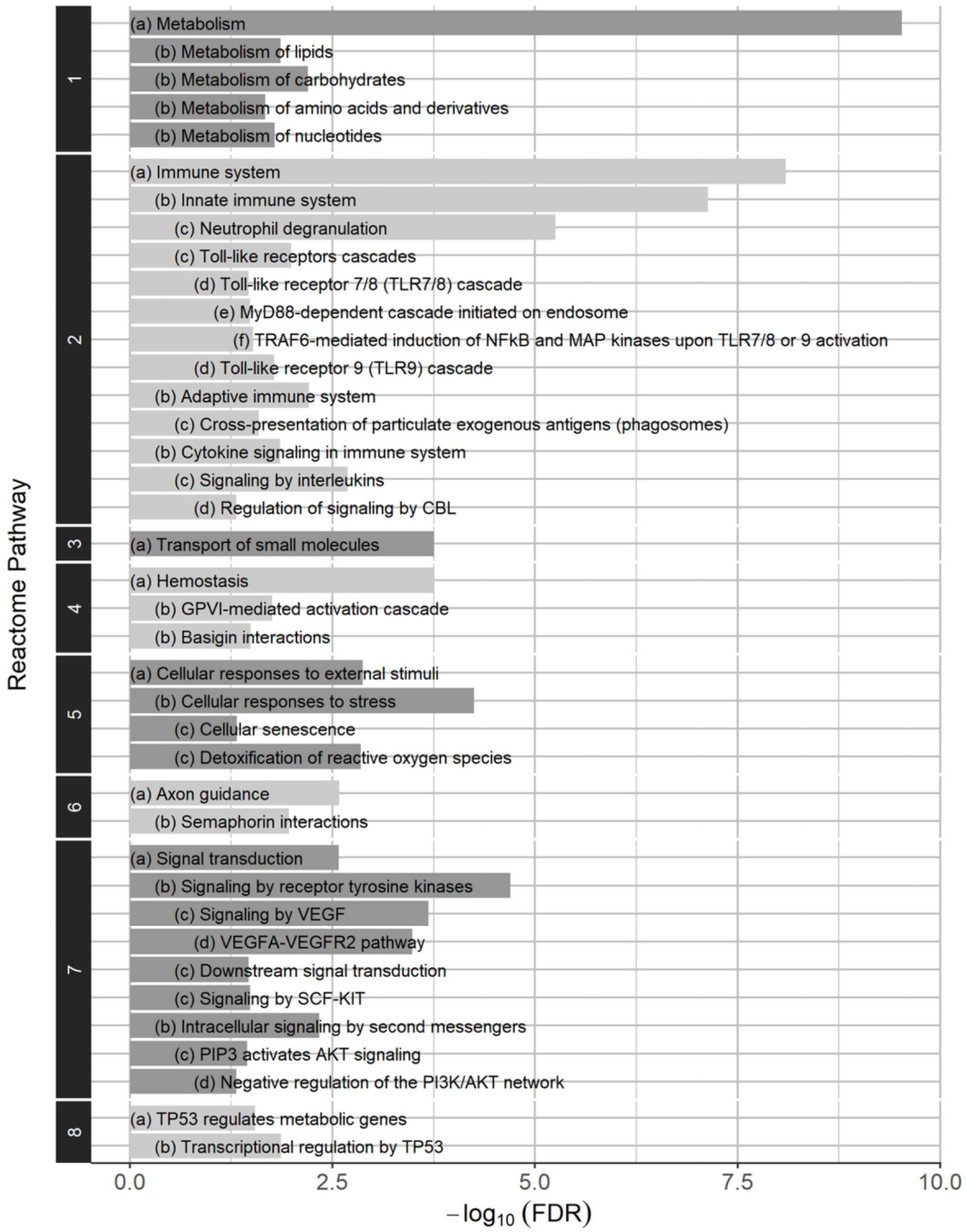

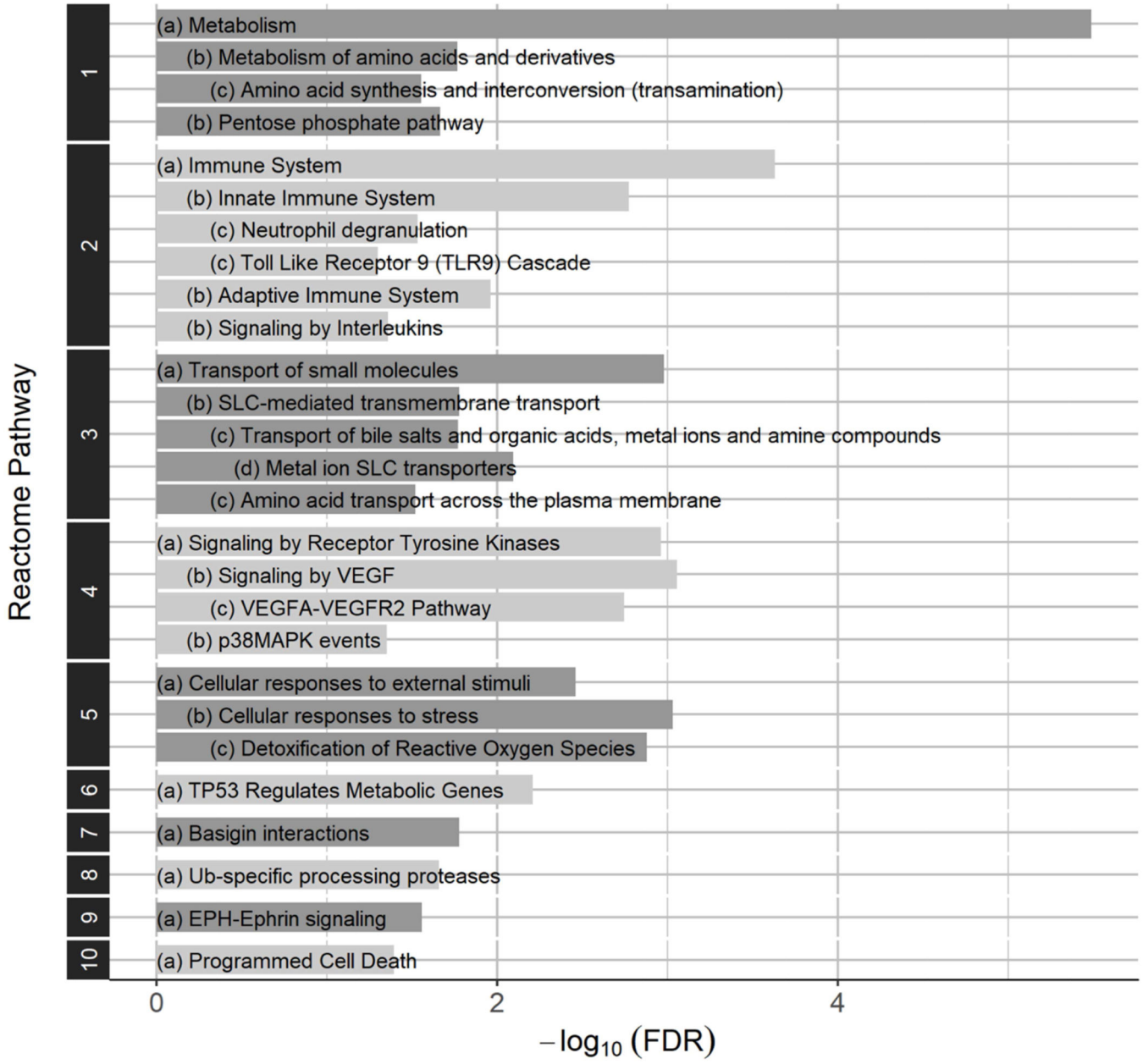

Figure 2: Biological pathways in the Affymetrix data.

Reactome pathways dysregulated in peritoneal macrophages treated with DEPe, based on Affymetrix data. **(A)** Reactome pathways of all DEGs (749), grouped by pathway sets numbered 1 through 8. The sets are represented by the following parental pathways: (1) metabolism, (2) immune system, (3) transport of small molecules, (4) hemostasis, (5) cellular responses to external stimuli, (6) developmental biology, (7) signal transduction, and (8) gene expression (transcription). **(B)** Reactome pathways of the upregulated genes (379), grouped by pathway sets numbered 1 through 10. The sets are represented by the following parental pathways: (1) metabolism, (2) immune system, (3) transport of small molecules, (4) signal transduction, (5) cellular responses to external stimuli, (6) gene expression (transcription), (7) hemostasis, (8) metabolism of proteins, (9) developmental biology, and

(10) programmed cell death. For both figures in **(A)** and **(B)**, the top-most hierarchical pathways are labeled with “(a)”, followed by its sub-level pathways labeled with “(b)” to “(f)”. Pathway sets are in descending order (top to bottom) of the $-\log_{10}$(FDR) of each set’s top-most hierarchical term.

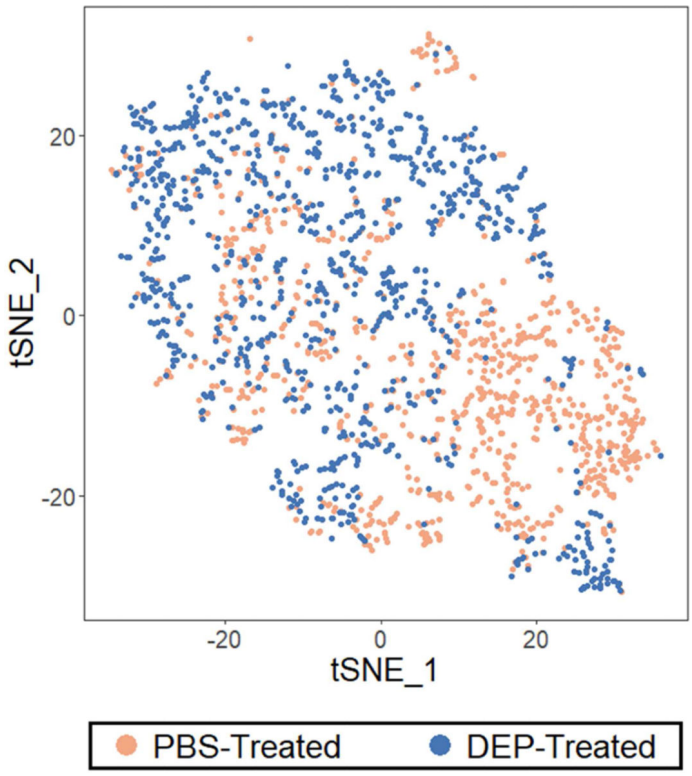

Figure 3: Alveolar macrophage clustering.

t-SNE (t-distributed stochastic neighbor embedding) plot of the scRNA-seq clusters of alveolar macrophages from PBS-treated vs. DEP-treated mice. Clustering was done based on the list of 109 genes that were significantly differentially expressed between the two groups, using five principal components (PCs).

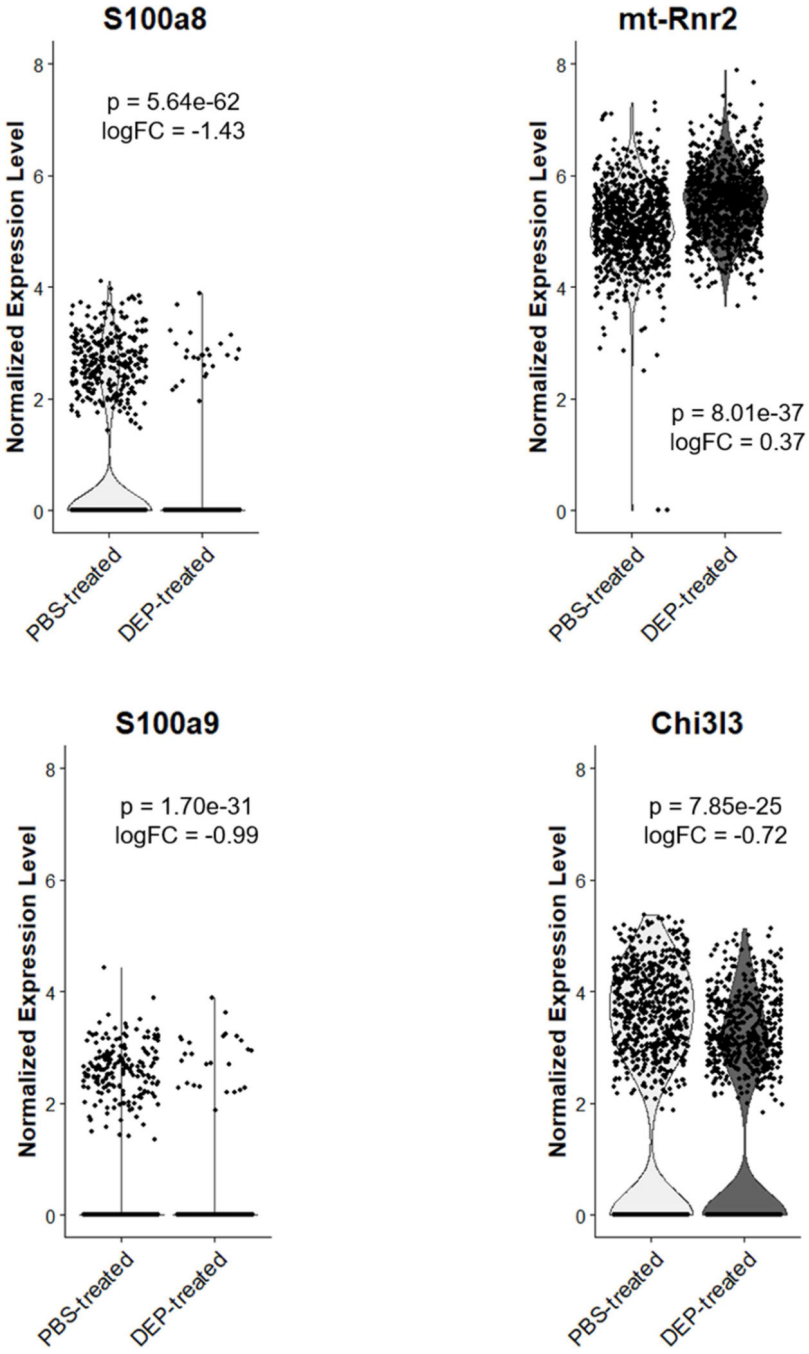

Figure 4: Alveolar macrophage gene expression.

Violin plots for the mRNA expression of the top four DEGs (FDR < 0.05) in alveolar macrophages from the scRNA-seq dataset (Table 2). The logFC refers to the natural logarithm of the fold change between DEP-treated vs. PBS-treated cells.

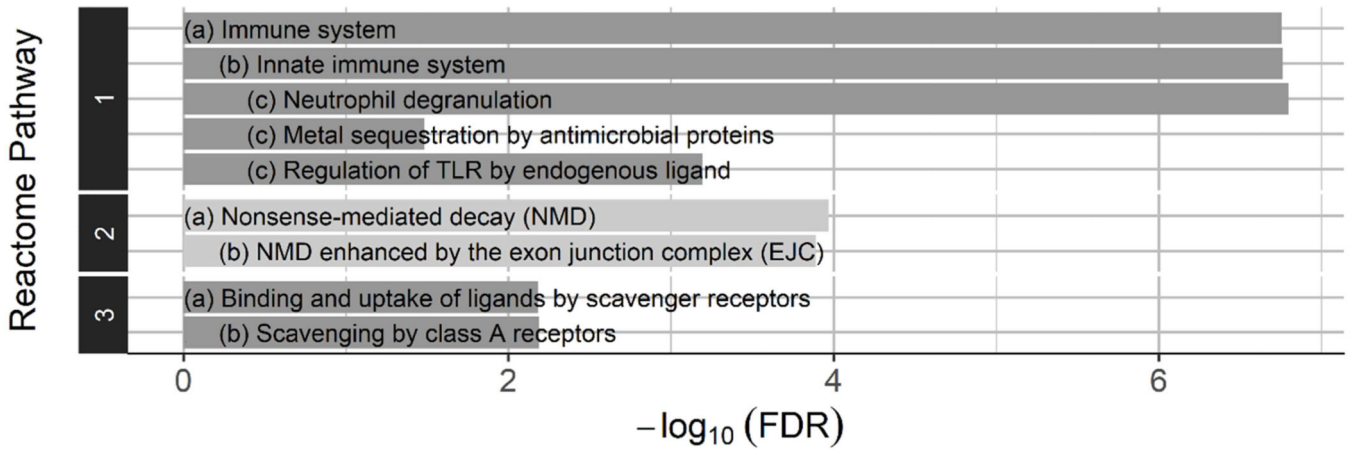

Figure 5: Biological pathways in the scRNA-seq dataset.

Nine Reactome biological pathways were dysregulated in alveolar macrophages of mice exposed to DEP compared with PBS. Reactome pathways of all DEGs (109) are grouped by pathway sets numbered 1 through 3. The sets are represented by the following parental pathways: (1) immune system, (2) metabolism of RNA, and (3) vesicle-mediated transport. The top-most hierarchical pathways are labeled with "(a)", followed by its sub-level pathways labeled with "(b)" to "(c)". Pathway sets are in descending order (top to bottom) of the -$\log_{10}$(FDR) of each set's top-most hierarchical term.

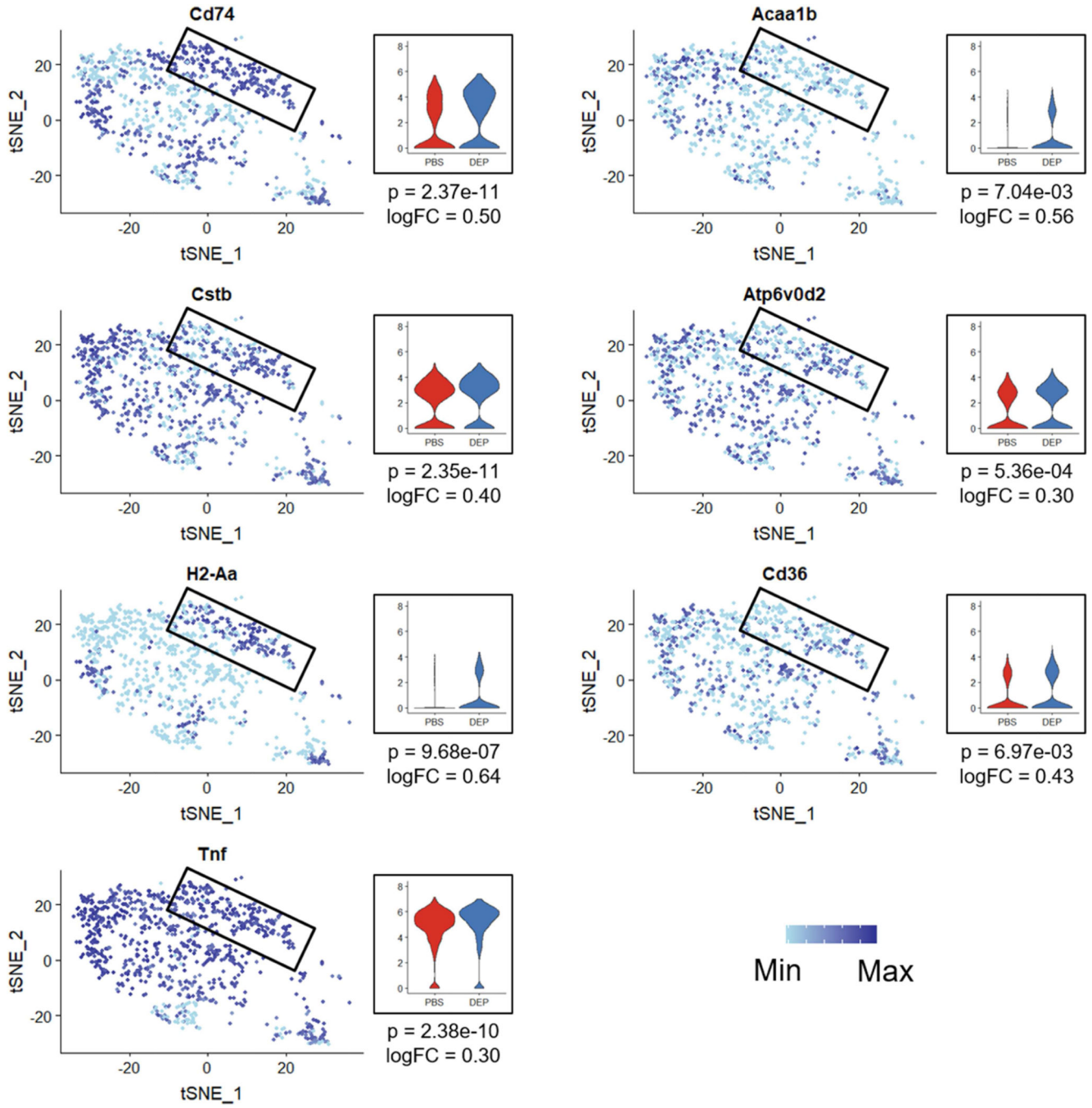

Figure 6: Alveolar macrophages exhibit heterogeneous gene expression among immune-related genes.

tSNE plots of mRNA expression levels in alveolar macrophages from DEP-treated mice of select immune system pathway genes. The seven genes shown were significantly upregulated in DEP-treated vs. PBS-treated mice. They also exhibited large variation among individual cells (inter-cell heterogeneity). Each dot in the tSNE plots represents a cell in the DEP-treated group. The boxed region in each plot represents an example in which there are a subset of cells with higher expression of four genes on the left column and lower expression of the other three genes in the right column (intra-cell heterogeneity). The color

gradient from light to dark blue colored dots represent the minimum and the maximum expression value, respectively, for that gene. Violin plots of the PBS- vs. DEP-treated groups are included for each gene, with the adjusted p-value and logFC listed underneath each violin plot. The logFC refers to the natural logarithm of the fold change between DEP-treated vs. PBS-treated.

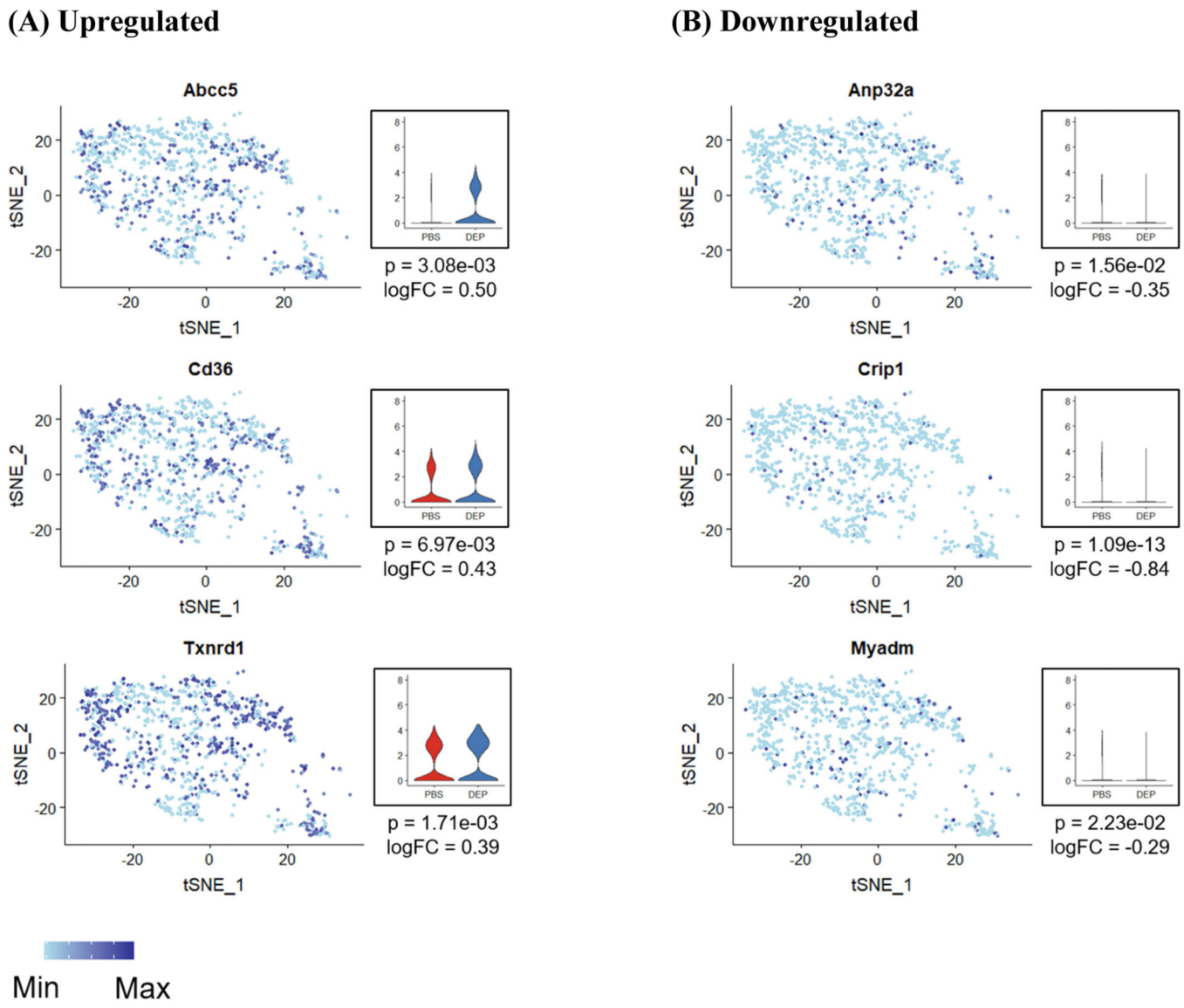

Figure 7: Expression of genes commonly dysregulated in the Affymetrix and scRNA-seq datasets.

tSNE plots of expression levels in alveolar macrophages from DEP-treated mice of the six genes that were commonly dysregulated in Affymetrix and scRNA-seq datasets, from Table 5. **(A)** The genes on the left side were all upregulated in both platforms, while **(B)** the genes on the right side were all downregulated in both platforms. Each dot represents an alveolar macrophage in the DEP-treated group from the scRNA-seq data. The color gradient from light to dark blue colored dots represent the minimum and the maximum expression value, respectively, for that gene. Violin plots of the PBS- vs. DEP-treated groups are included for each gene, with the adjusted p-value and logFC listed underneath each violin plot. The logFC refers to the natural logarithm of the fold change between DEP-treated vs. PBS-treated.

Table 1:

DEGs in the Affymetrix dataset.

	Gene	Name	log_2(FC)	FDR
1	Hmox1	heme oxygenase (decycling) 1	3.32	1.75E-06
2	Slc40a1	solute carrier family 40 (iron-regulated transporter), member 1	3.40	1.75E-06
3	Gclm	glutamate-cysteine ligase, modifier subunit	3.51	1.75E-06
4	Srxn1	sulfiredoxin 1 homolog (S. cerevisiae)	3.33	1.75E-06
5	Abcc1	ATP-binding cassette, sub-family C (CFTR/MRP), member 1	2.98	1.75E-06
6	Gdf15	growth differentiation factor 15	2.48	5.97E-06
7	Ednrb	endothelin receptor type B	2.46	6.86E-06
8	Gclc	glutamate-cysteine ligase, catalytic subunit	2.25	1.38E-05
9	Txnrd1	thioredoxin reductase 1	2.72	1.68E-05
10	Ikbkg	inhibitor of kappaB kinase gamma	2.13	1.68E-05
11	P2ry6	pyrimidinergic receptor P2Y, G-protein coupled, 6	−2.14	1.68E-05
12	Ehd1	EH-domain containing 1	2.14	2.09E-05
13	Themis2	thymocyte selection associated family member 2	−2.03	2.20E-05
14	Tshz1	teashirt zinc finger family member 1	1.98	2.55E-05
15	Trib3	tribbles homolog 3 (Drosophila)	2.10	3.51E-05
16	Coro1a	coronin, actin binding protein 1A	−1.85	3.51E-05
17	Slc7a11	solute carrier family 7 (cationic amino acid transporter, y+ system), member 11	2.88	3.75E-05
18	Enc1	ectodermal-neural cortex 1	−2.56	4.83E-05
19	Ptgr1	prostaglandin reductase 1	1.88	5.19E-05
20	Cbr3	carbonyl reductase 3	1.95	5.45E-05
21	Mafb	v-maf musculoaponeurotic fibrosarcoma oncogene family, protein B (avian)	−1.73	5.45E-05
22	Spred2	sprouty-related EVH1 domain containing 2	2.12	5.45E-05
23	Itpkb	inositol 1,4,5-trisphosphate 3-kinase B	−1.70	5.45E-05
24	Id3	inhibitor of DNA binding 3	−2.11	6.02E-05
25	Panx1	pannexin 1	1.63	8.21E-05
26	Asns	asparagine synthetase	1.59	8.86E-05
27	Procr	protein C receptor, endothelial	1.61	1.06E-04
28	Vps37b	vacuolar protein sorting 37B (yeast)	1.81	1.18E-04
29	Met	met proto-oncogene	1.78	1.18E-04
30	Ampd3	adenosine monophosphate deaminase 3	2.28	1.20E-04
31	Mthfd2	methylenetetrahydrofolate dehydrogenase (NAD+ dependent), methenyltetrahydrofolate cyclohydrolase	1.79	1.21E-04
32	Kcnn4	potassium intermediate/small conductance calcium-activated channel, subfamily N, member 4	−1.58	1.21E-04
33	Cxcl2	chemokine (C-X-C motif) ligand 2	1.65	1.21E-04
34	Ero1l	ERO1-like (S. cerevisiae)	1.51	1.30E-04
35	Nck2	non-catalytic region of tyrosine kinase adaptor protein 2	1.44	1.68E-04
36	Ralgds	ral guanine nucleotide dissociation stimulator	1.66	1.73E-04

	Gene	Name	log_2(FC)	FDR
37	Dbp	D site albumin promoter binding protein	−1.50	1.79E-04
38	Tcfec	transcription factor EC	1.67	1.80E-04
39	Ikbke	inhibitor of kappaB kinase epsilon	−1.45	1.85E-04
40	Clec4n	C-type lectin domain family 4, member n	1.43	1.90E-04

Table includes the top 40 DEGs in DEPe-treated peritoneal macrophages vs. controls, identified from Affymetrix data, listed in descending order of FDR values. The log_2(FC) refers to the logarithm (base 2) of the fold change of DEP-treated vs. PBS-treated.

Table 2:

KEGG pathways of the 749 DEGs from the Affymetrix dataset.

Pathway	FDR
Chemokine signaling pathway	4.15E-05
Central carbon metabolism in cancer	3.22E-03
HTLV-I infection	6.04E-03
B cell receptor signaling pathway	7.18E-03
Toll-like receptor signaling pathway	1.64E-02
Glutathione metabolism	1.68E-02
Aminoacyl-tRNA biosynthesis	1.69E-02
HIF-1 signaling pathway	1.80E-02
Biosynthesis of antibiotics	2.41E-02
TNF signaling pathway	3.27E-02
Choline metabolism in cancer	4.84E-02
Cytosolic DNA-sensing pathway	4.85E-02

KEGG pathways are listed in descending order of the FDR.

Table 3:

BioCarta and KEGG pathways of the 379 upregulated DEGs from the Affymetrix dataset.

Pathway	FDR
Aminoacyl-tRNA biosynthesis (KEGG)	8.22E-05
Glutathione metabolism (KEGG)	6.32E-03
Oxidative stress-induced gene expression via Nrf2 (BioCarta)	1.35E-02

Pathways are listed in descending order of the FDR.

Table 4:

DEGs in the scRNA-seq dataset.

	Gene	Name	log(FC)	FDR
1	S100a8	S100 calcium binding protein A8 (calgranulin A)	−1.43	5.64E-62
2	mt-Rnr2	16S rRNA, mitochondrial	0.37	8.01E-37
3	S100a9	S100 calcium binding protein A9 (calgranulin B)	−0.99	1.70E-31
4	Chi3l3	Chitinase-like 3	−0.72	7.85E-25
5	Tmsb4x	Thymosin, beta 4, X chromosome	−0.31	1.64E-18
6	Vim	Vimentin	−0.60	2.31E-16
7	Tppp3	Tubulin polymerization-promoting protein family member 3	−0.84	4.75E-15
8	Calr	Calreticulin	−0.49	1.53E-14
9	Hbb-bs	Hemoglobin, beta adult s chain	−0.75	9.75E-14
10	Crip1	Cysteine-rich protein 1 (intestinal)	−0.84	1.09E-13
11	Hspa5	Heat shock protein 5	−0.33	2.18E-12
12	Hsp90b1	Heat shock protein 90, beta (Grp94), member 1	−0.36	7.93E-12
13	Cstb	Cystatin B	0.40	2.35E-11
14	Cd74	CD74 antigen (invariant polypeptide of major histocompatibility complex, class II antigen-associated)	0.50	2.37E-11
15	Tagln2	Transgelin 2	−0.40	3.22E-11
16	Malat1	Metastasis associated lung adenocarcinoma transcript 1 (non-coding RNA)	−0.26	3.45E-11
17	Hspa8	Heat shock protein 8	−0.49	8.72E-11
18	Tnf	Tumor necrosis factor	0.30	2.38E-10
19	mt-Rnr1	12S rRNA, mitochondrial	0.39	9.13E-10
20	Lyz2	Lysozyme 2	−0.37	1.54E-09
21	Ctsc	Cathepsin C	−0.43	1.90E-09
22	Cd9	CD9 antigen	−0.30	2.63E-09
23	Gpx1	Glutathione peroxidase 1	−0.42	4.28E-09
24	Spp1	Secreted phosphoprotein 1	−0.40	3.09E-08
25	Rpl41	Ribosomal protein L41	−0.45	4.47E-08
26	Plet1	Placenta expressed transcript 1	−0.34	1.32E-07
27	Tyrobp	TYRO protein tyrosine kinase binding protein	−0.43	2.09E-07
28	Gm10800		0.68	2.55E-07
29	Klf6	Kruppel-like factor 6	−0.46	3.14E-07
30	H2-Aa	Histocompatibility 2, class II antigen A, alpha	0.64	9.68E-07
31	BC005537	cDNA sequence BC005537	0.32	3.06E-06
32	Rps29	Ribosomal protein S29	−0.39	5.64E-06
33	Spcs2	Signal peptidase complex subunit 2 homolog (S. cerevisiae)	−0.46	5.66E-06
34	Ptma	Prothymosin alpha	−0.39	5.75E-06
35	Gda	Guanine deaminase	−0.36	2.69E-05
36	Myl6	Myosin, light polypeptide 6, alkali, smooth muscle and non-muscle	−0.42	2.79E-05

	Gene	Name	log(FC)	FDR
37	Pdia3	Protein disulfide isomerase associated 3	−0.37	2.79E-05
38	Rps19	Ribosomal protein S19	−0.43	2.85E-05
39	Rps28	Ribosomal protein S28	−0.44	3.30E-05
40	Cox6c	Cytochrome c oxidase subunit 6C	−0.40	3.73E-05

Table includes the top 40 differentially expressed genes in alveolar macrophages from the DEP-treated group vs. the PBS-treated group, identified from scRNA-seq data, listed in descending order of FDR values. The log(FC) refers to the natural logarithm of the fold change of DEP-treated vs. PBS-treated.

Table 5:

Common DEGs in the Affymetrix and scRNA-seq datasets.

	Gene Name	log_2(FC) in Affymetrix Data	log(FC) in scRNA-seq Data
Abcc5	ATP-binding cassette, sub-family C (CFTR/MRP), member 5	0.50	0.50
Anp32a	Acidic (leucine-rich) nuclear phosphoprotein 32 family, member A	−0.88	−0.35
Cd36	CD36 molecule	1.21	0.43
Crip1	Cysteine-rich protein 1 (intestinal)	−0.68	−0.84
Ctsc	Cathepsin C	0.62	−0.43
Fabp4	Fatty acid binding protein 4, adipocyte	−1.03	0.59
Hsp90aa1	Heat shock protein 90, alpha (cytosolic), class A member 1	0.75	−0.32
Klf6	Kruppel-like factor 6	0.52	−0.46
Mmp19	Matrix metallopeptidase 19	0.55	−0.47
Myadm	Myeloid-associated differentiation marker	−0.59	−0.29
Txnrd1	Thioredoxin reductase 1	2.72	0.39

Table includes the 11 genes that were significantly differentially expressed in both the Affymetrix and scRNA-seq data. The genes *Cd36*, *Ctsc*, and *Hsp90aa1* were also commonly found in the immune system, innate immune system, and neutrophil degranulation pathways in both datasets. The log_2(FC) refers to the logarithm (base 2) of the fold change of DEP-treated vs. PBS-treated in Affymetrix data while log(FC) refers to the natural logarithm of the fold change of DEP-treated vs. PBS-treated in scRNA-seq data.